



Licorice (*Glycyrrhiza glabra*) as corrosion inhibitor of carbon steel reinforcing bars in mortar and its synergic effect with nitrite



R. Naderi^a, A. Bautista^{b,*}, S. Shagñay^b, F. Velasco^b

^a School of Metallurgy and Materials Engineering, College of Engineering, University of Tehran, Tehran, Iran

^b Department of Materials Science and Engineering, IAAE, Universidad Carlos III de Madrid, Avda. Universidad 30, 28911 Leganés, Madrid, Spain

ARTICLE INFO

Article history:

Received 5 May 2023

Revised 30 August 2023

Accepted 14 September 2023

Available online 19 September 2023

Keywords:

Corrosion

Reinforcing steel

Green inhibitor

EIS

Mechanical test

Polarization

Chlorides

ABSTRACT

Nitrites are effective corrosion inhibitors for concrete structures, but their toxicity leads to their total or partial substitution. Licorice and its synergic effect with nitrites are studied both in simulated pore solutions and in mortars with chlorides. EIS and polarization studies show that a 50% licorice + 50% Na₂NO₂ mix can reduce the corroding surface and the corrosion rate in solution. Moreover, the efficiency of this mix is higher than that of Na₂NO₂ when it is added to mortars with 0.8% Cl⁻. The tested inhibitors, in the amount considered (0.2%), do not affect the mechanical properties of the mortars.

© 2023 The Author(s). Published by Elsevier B.V. on behalf of The Korean Society of Industrial and Engineering Chemistry. This is an open access article under the CC BY-NC-ND license (<http://creativecommons.org/licenses/by-nc-nd/4.0/>).

Introduction

Concrete is the building material par excellence. It provides chemical protection to steel, as its alkaline pH passivates it. However, the alkaline compounds in concrete tend to react with atmospheric CO₂ [1], so the durability of structures can be compromised. Furthermore, the depassivating ions in the environment (chlorides) can locally break the passivity of the steel [2,3], causing pitting corrosion of the bars, which is usually more aggressive than the corrosion caused by carbonation.

The products that the reinforcements generate when they corrode have a much higher volume than metal, so they generate tensile stresses in the concrete cover. This easily leads to its cracking and detachment, especially for corrosion mass losses greater than 2.4% [3,4]. Moreover, corrosion reduces the section of the steel reinforcement and affects its mechanical resistance [5]. For all these reasons, the corrosion of the steel is the main cause of deterioration of reinforced concrete structures located in aggressive environments and is behind the catastrophic failure of structures when mechanical stresses are added to its detrimental effect.

The hindering of corrosion of the reinforcements must be guaranteed in the design stage by using high quality, dense concrete

with an adequate thickness cover [6], cathodic protection of the steel reinforcements [7] or by using stainless steel bars in the most exposed areas of the structure [8,9]. Moreover, the use of inhibitors in concrete formulations is considered another interesting option for controlling corrosion of reinforcements.

Various corrosion inhibitors have been employed to date, among which the nitrite-based compounds have a long history in this field due to their excellent performance [10]. These concrete-compatible compounds, playing the role of passivator, are reported to be able to inhibit chloride and carbonation-induced corrosion of steel reinforcements [11]. In fact, the nitrite-based anodic inhibitors can stabilize the surface oxide layer with no contribution to its composition [12]. Nitrites are assumed to compete with chlorides in the reaction with the ferrous ions and favor the oxidation of the Fe²⁺ cation into stable films, while they are reduced to NO [13]. Nitrite-based inhibitors have been reported to be the most efficient in preventing the corrosion induced by chlorides in concrete [14]. For instance, they have been proved to be more effective than other inorganic passivating compounds such as phosphates [6]. At the same time, sodium nitrites have been determined to be the most effective nitrites for reducing the corrosion of reinforcing steel, followed by potassium nitrites and then by calcium nitrites [15]. However, nitrites are considered toxic [14], and calcium nitrites shorten the setting time and increase the drying shrinkage [16].

* Corresponding author.

E-mail address: mbautist@ing.uc3m.es (A. Bautista).

Restrictions on the use of nitrites due to environmental issues have led to widespread efforts to replace them, at least partially, and interesting contributions in this line can be found in the literature. Okeniyi *et al.* demonstrated an inhibition synergism between NaNO_2 and triethanolamine ($\text{C}_6\text{H}_{15}\text{NO}_3$) on the corrosion of steel reinforcement in concrete exposed to sodium chloride and sulfuric acid solutions, with the advantage of reducing the adverse environmental impacts for lower NaNO_2 content [17]. In simulated concrete pore solution tests, the corrosion inhibitor, composed of environment-friendly sodium D-gluconate with nitrite, proposed by Xu *et al.* for carbon steel bars, has shown a significant impact on reducing the number and area of pitting corrosion [18]. Johari *et al.* examined the simultaneous use of trisodium citrate, sodium–potassium tartrate and sodium nitrite to provide an effective corrosion inhibitor mixture containing low nitrite content for carbon steel bars, also resorting exclusively to the simulated concrete pore solution test [19].

Another strategy is to completely replace the toxic inhibitors using only green corrosion inhibitors, such as plant extracts, which are mainly composed of the organic molecules enriched with N, O, S heteroatoms and different functional groups [20–23]. These green inhibitors have been mainly tested in acid [24,25]. Various plant extracts, e.g. Rosa damascena leaf [26], ginger [27], turmeric [28], *Chamaerops Humilis* L. leaves [29], *Olea europaea* L. [30], *Platanus acerifolia* leaf [31], *Fatsia Japonica* leaves [32], *Eucalyptus Globulus*, *Punica Granatum*, and *Olea Europaea* [33], have already been proved to enhance the steel reinforcement corrosion resistance in simulated concrete pore solution. Moreover, the inhibiting ability of some extracts has begun to be explored in concrete. Along these lines, *Ricinus communis* [34] reduces the steel corrosion rate through a mixed type inhibition, modifying reactions of both cathodic and anodic sites. Green tea extract promotes precipitation of calcium carbonates in concretes under impressed current, being able to enhance the inhibiting efficiency of nitrites [35]. Synergism of plant extracts (rosemary) with traditional inhibitors (ZnCl_2) has been checked in saline environments [36].

From the economic, industrial and scientific point of view, licorice (*Glycyrrhiza glabra*) has attracted a good deal of attention due to its sweet taste, pharmacological properties and high nutritional value. In the field of corrosion protection, some reports can be found indicating the robust corrosion inhibition efficiency of licorice extract, including a variety of species (e.g. glycyrrhizin, glycyrrhetic acid, flavonoids, liquiritigenin, licochalcone and glabridin) [37–39], on steel specimens in aggressive electrolytes with different pHs [40,41].

Taking advantage of electrochemical methods, this work aims to assess the potential of the extract of licorice as an environmentally-friendly corrosion inhibitor for carbon steel reinforcements to totally or partially replace sodium nitrite, when the inhibitory additions are used to reduce the corrosion rate of carbon steel reinforcement in active state. Maintaining the good mechanical properties of the mortars while reducing the corrosion rate of the steel reinforcing bars in chloride contaminated environments has been considered an important goal in this study.

In our previous work, focused on the corrosion behavior on the ribbed steel bars dipped into the chloride-polluted simulated concrete pore solution [38], the green licorice dosage that provided the most effective corrosion inhibition was determined. However, the possibility that there are synergies between the inhibitory mechanism of this licorice and that of nitrites under these conditions has not been explored yet. Moreover, results obtained in solution need to be checked in mortar, as factors such as oxygen access to the bar or the complex morphology of the mortar/concrete interface can affect them.

The compatibility of the inhibitory additions with the cured mortar is another innovative point that must also be checked, as

key factor for future in-service use. Some previous studies about corrosion inhibitors -different from licorice- inform about changes in the microstructure [42] and decrease on the mechanical properties [14,43] of the concretes when they are added. The present article addresses the study of the effect of licorice and licorice + nitrite mixes in the mechanical properties and porosity of the mortars, which is a topic that has not been studied yet.

Experimental

The licorice extract tested as inhibitor was obtained from the root of this plant by an aqueous method. The roots, after being dried at room-temperature, were pieced into small parts, and then stirred in water at 70 °C for 3 h. The obtained solution was filtered, and dried in an oven at 60 °C for 24 h to obtain the extract tested as the corrosion inhibitor for carbon steel reinforcements.

The 8-mm diameter TMT carbon steel ribbed bars, B500 type, were used to carry out the solution corrosion test as well as the corrosion test in mortar. The chemical composition of the ribbed steel is shown in Table 1.

Solution test

For simulating the concrete pore solution in the corrosion test, a 3 M KOH + 0.1 M NaOH solution was saturated with Ca(OH)_2 [44,45]. Corrosion inhibitors (licorice and/or sodium nitrite) were also added to this solution before the immersion of the carbon steel bar. Solutions were prepared with 0.1% by weight of inhibitor, as was determined in previous studies [38]. At this concentration, licorice remains completely soluble in the alkaline simulated pore solution. The solution remained clear and not precipitation of sediments took place. However, precipitation was found for 0.2% by wt. The inhibitor composition ranged from 100% licorice (labelled as Lic0.1%) to 100% sodium nitrite (labelled as SN0.1%), including three mixtures of both of them (SN25-Lic75, SN50-Lic50, and SN75-Lic25). The solution tests involved the immersion of the bars in the inhibited simulated concrete pore solutions to allow the formation of a passivating film on the bars. After 1 h, 1 wt. % NaCl (0.6% Cl^-) was added to the simulated pore solutions. Moreover, reference bars (blank specimens) were also tested in the simulated pore solution with NaCl and without the inhibitor addition.

The inhibitory ability of the five solutions was studied through electrochemical impedance spectroscopy (EIS) and polarization curves. A traditional three-electrode cell was employed for both types of electrochemical measurements. Carbon steel reinforcement bars were used as the working electrodes (WE), stainless-steel spiral wires around the WE acted as the counter electrodes (CE); and a saturated calomel electrode (SCE) was employed as reference electrode (RE). The region of the WE bars around to the solution/air interface were sealed with epoxy paint with the aim of preventing the formation of differential aeration cells that could affect the results. The immersed cross-sections of the bars were also sealed with epoxy, as the core of the steel had a ferritic-perlitic microstructure with a different corrosion resistance than the martensite forming the outermost part of the TMT bars [3]. After these treatments, an area of 3-cm in length of the WE were delimited to be exposed to the different testing electrolyte. Gamry Reference 600 potentiostat/galvanostat was used to carry out both types of measurements (EIS and polarization curves).

EIS were recorded at open circuit potential (OCP) applying a voltage sinusoidal perturbation of 10 mV. The measurements were carried out using 6 points per decade from a frequency of 10^5 Hz down to a frequency 5 mHz. The EIS spectra were acquired after 2, 5 and 24 h immersion of the WE in the simulated pore solutions (that is to say, 1, 4 and 23 h after the chloride addition). Three sam-

Table 1
Chemical composition of the reinforcing ribbed bars used for the solution and mortar corrosion test (% by weight).

C	S	P	Si	Mn	Cr	Cu	Mo	Ni	Fe
0.13	0.022	0.006	0.23	0.54	0.15	0.44	0.02	0.12	Bal.

ples were evaluated in each one of the 6 solutions considered in the study, and the numerical data shown in the present study are averaged values of the 3 measurements. To fit the experimental spectra obtained, Zview software was used.

Polarization measurements were carried out in some samples after the EIS measurements to obtain complementary information about the corrosion mechanism and kinetics. The measurements at – 300 mV vs. OCP and finished at + 300 mV vs. OCP. The potential sweeping rate was 1 mV/s.

Mortar samples

Portland cement IV was selected for mortar manufacturing. The water/cement ratio (L/S) was 0.5, and the cement to standard sand (with 0.08–2 mm of grain size) ratio was 1:3. Mortars with different inhibitory additions were manufactured and compared to a blank sample, without any corrosion inhibitor (labelled as CEM IV). The inhibited mortars considered contained 0.1% and 0.2% of licorice by wt. in relation to cement (labelled as CEM IV + 0.1Lic and CEMIV + 0.2Lic, respectively), 1% licorice and 0.1% sodium nitrite (labelled as CEM IV + 0.1Lic + 0.1SN) and with 0.2% sodium nitrite (labelled as CEM IV + 0.2SN). The amount of inhibitors added was limited so as not to affect the mechanical properties of the mortar. During the first exploratory tests, it was been checked in our laboratory that adding amounts of licorice as high as 0.4% already interferes in the curing reactions of the cement, so additions higher than 0.2% were left out the final experimental design.

Non-reinforced samples of each of the 5 types of mortars were manufactured. These samples had a prismatic shape and measured 4x3x16 cm. After curing at high RH (about 95%) and room temperature for 28 days, their compression and bending strength were measured. Both tests were carried out in quadruplicate, using a universal testing machine from Microtest and following the specifications of the UNE-EN 196 standard. For both tests, a load rate of 5 mm/min was used. The numerical results about mechanical properties shown in the present study for each mortar are averaged values of 4 measurements.

Hg porosity was measured for all mortars. This technique is based on the Washburn equation that relates the applied pressure to the diameter of the pore into which Hg is introduced. Information related to pore sizes between 4 nm and 200 μ m was obtained with the Poremaster-60 GT equipment of Quantachrome Instruments, exerting a pressure up to 400 MPa. Two samples were used to check the repeatability of the data for each mortar formulation.

Moreover, carbon steel reinforcements of 250 mm-length were embedded in cylindrical mortar samples to evaluate the effect on corrosion of licorice and the synergism between licorice and sodium nitrite. In Fig. 1a, a schema of the samples manufactured for this study is shown. In all cases, mortar samples had a fixed CaCl₂ amount in their composition. (1.25% by wt., which implies a 0.8% of chlorides in relation to the cement weight). This value duplicates the 0.4% limit required (according to EN 206 standard) usually assumed to keep the risk of corrosion low for the carbon steel reinforcements in concrete. According to NRMCA [46], the amount of added chlorides can be in the threshold concentration (~0.4 to 0.8% of the weight of cement) for corrosion to initiate at the reinforcing steel.

The embedded cross section of the carbon steel bar as well as the region close to the air mortar interface were blocked with an epoxy coating to avoid corrosion phenomena that could interfere in the measurements.

After the 28-day curing period, the electrochemical behavior of all reinforced mortar specimens was monitored. EIS studies were carried out, using a 3-electrode configuration, and an image of the placement of the electrodes during the EIS measurements in mortar can be seen in Fig. 1b. The non-coated surface of the carbon steel reinforcement embedded in the mortar acted as WE. A cylindrical brass CE is located surrounding the full reinforced mortar sample. The good contact between the CE and the mortars was assured with thin wet pads. A SCE RE was placed on the upper surface of the mortar close to the rebar, also using a wet pad to assure good electrical contact.

The cured samples were kept at 95% RH during 3 months for EIS monitoring. EIS testing was configured so that the frequency spectrum ranged from 10³ to 5·10⁻² Hz, using a perturbation sinusoidal signal with 10 mV of amplitude and acquiring 6 points per decade. The electrochemical monitoring was carried out using a multiplicity of 4 for all the 5 systems under study. The obtained spectra were analyzed using the Zview software and the numerical data shown in this article are averaged values obtained from the 4 samples of the same mortar manufactured for this study.

Results and discussion

Innovative experimental results were obtained in the development of this research, which comprises electrochemical tests in different solutions, characterization of mortars with inhibitors and an electrochemical study of the behavior of reinforced steel bars in mortar with inhibitors. The most relevant results obtained are summarized in the tables and figures of this contribution. They are always expressed as mean values with their standard deviations in the tables and using error bars in the figures.

Solution study of the effectiveness of simultaneous use of the two inhibitors

Simulated pore solutions with and without inhibitors were used to initially explore the synergism between licorice and nitrites. Chlorides were added to the solution after the first hour of immersion of the steel bars to allow the inhibitors to act on the steel surface.

As can be seen in Fig. 2, after 2 h, the steel in the blank solutions has an OCP whose values are clearly in the active corrosion region defined by the ASTM C876 standard for steel in concrete. Meanwhile, for the solutions with inhibitors, the OCP is > -275 mV vs. SCE, that is to say, they are still in the corrosion uncertainty region. For sodium nitrite reference inhibitors, the [NO₂]/[Cl⁻] molar ratios proposed in the literature to keep the passivity range between 0.5–1.5 [10,13]. The ratio used in the present study, whose objective is exploring the feasibility of the additions for reducing the corrosion rate, is lower than those reported values, so the results in Table 2 are foreseeable.

The OCP in all the studied solutions with chlorides becomes more negative as the immersion times extend, but the OCP of the steel in the blank solution is always more negative than those of the solutions with inhibitors. This indicates that the mechanisms

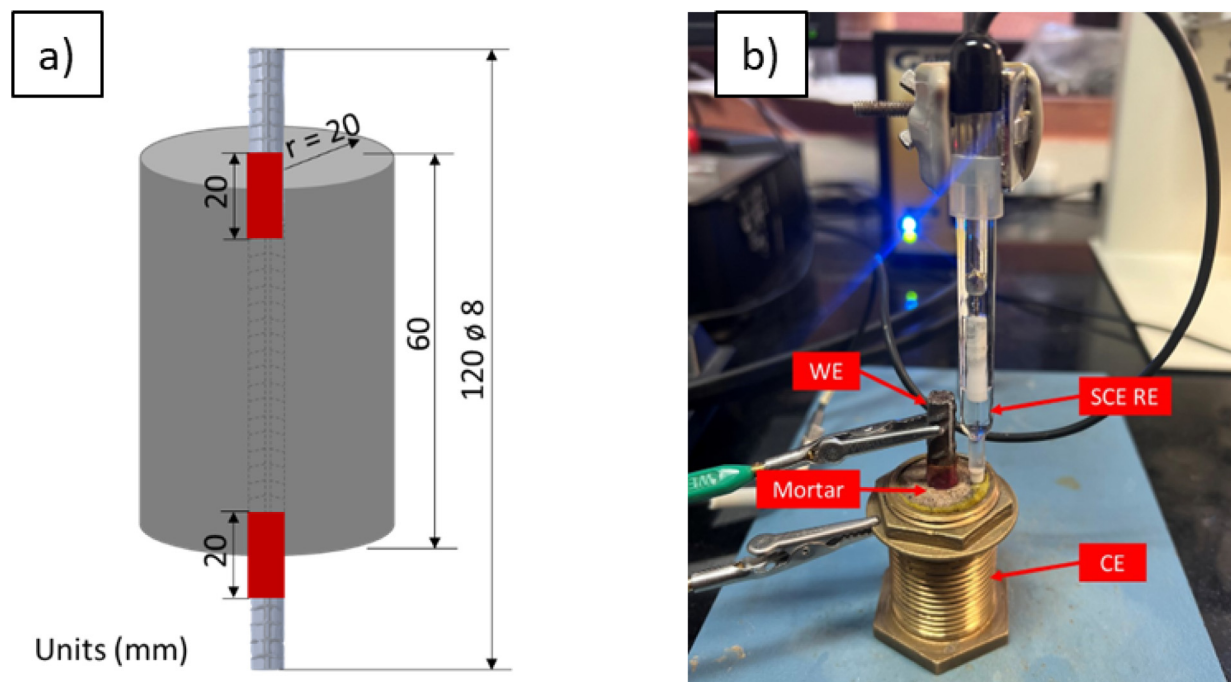


Fig. 1. Mortar reinforced samples used for the electrochemical measurements: a) schema of the samples manufactured; b) image of experimental set-up used for EIS monitoring.

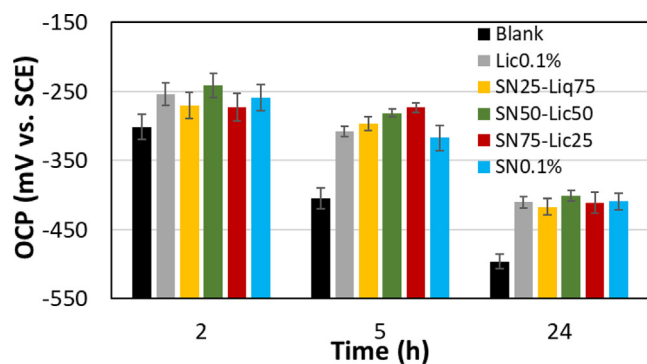


Fig. 2. OCP determined for the corrugated steels after different immersion times in solutions with and without inhibitors.

acting in the licorice and nitrite must be essentially anodic, as they cause increases in the OCP. Moreover, the difference between the OCP of the steel in inhibited and blank simulated pore solutions with chlorides tends to increase during the first hours of exposure, highlighting the effect of the inhibitors on corrosion development.

The corrosion kinetics and its evolution with time have been studied by EIS. The impact of nitrite-licorice ratio on the corrosion behavior of the bare steel bars in the simulated concrete pore solutions contaminated with sodium chloride can be seen in the examples plotted in Fig. 3.

Table 2

Parameters calculated from the polarization curves measured in different solutions.

	i_{corr} ($\mu\text{A}\cdot\text{cm}^{-2}$)	Mass loss rate ($\text{mg}\cdot\text{year}^{-1}\cdot\text{cm}^{-2}$)	E_{corr} (V vs SCE)	$ \beta_a $ (mV)	$ \beta_c $ (mV)
Blank	35 ± 9	3.7 ± 0.9	-0.48 ± 0.03	345 ± 9	240 ± 7
Lic0.1%	7 ± 3	0.7 ± 0.3	-0.42 ± 0.02	375 ± 9	235 ± 9
SN50-Lic50	6 ± 3	0.6 ± 0.3	-0.39 ± 0.03	350 ± 8	230 ± 7
SN0.1%	11 ± 4	1.2 ± 0.4	-0.44 ± 0.02	310 ± 8	245 ± 5

The AC impedance spectra, with a one-time constant appearance, were quantitatively assessed using a $R_s(R_{ct}CPE_{dl})$ equivalent circuit. The fitted spectra obtained using this circuit are plotted with continuous lines in the graphs in Fig. 3. In the simple equivalent circuit, the elements R_s , R_{ct} and CPE_{dl} are, respectively, the alkaline electrolyte resistance, the charge transfer resistance and the double layer constant phase element (defined by the admittance, Y_{dl} , and the exponent, n_{dl}). The R_{ct} , Y_{dl} and n_{dl} values obtained from the simulation of the experimental are shown in Fig. 4. The mean values obtained for χ^2 for the fitting of the spectra carried out in the different solution range from $(7.9 \pm 1.5) \cdot 10^{-4}$ to $(1.6 \pm 0.9) \cdot 10^{-3}$, which is coherent with the good correlation observed in the examples in Fig. 3 between experimental data and fitted data.

It can be observed that, for a given solution composition, R_{ct} decreases with immersion time (Fig. 4a), which informs about corrosion rates that always increase with time. This increase in the corrosion rate is coherent with the development of the pitting attack on the surface of bars, which typically has an autocatalytic mechanism. This mechanism that occurs in alkaline media in the presence of chlorides has been previously detailed in other work [2]. The decrease of the OCP with time observed in Fig. 3 is also coherent with this mechanism. The inhibitory mechanisms of licorice [38] and nitrites [47] are based on different chemical processes and both have been previously described in other studies. It is well-known that nitrites promote the formation of more protective oxides [48], while licorice, as is expected for organic inhibitors, precipitates on the surface, preferentially blocking the anodic

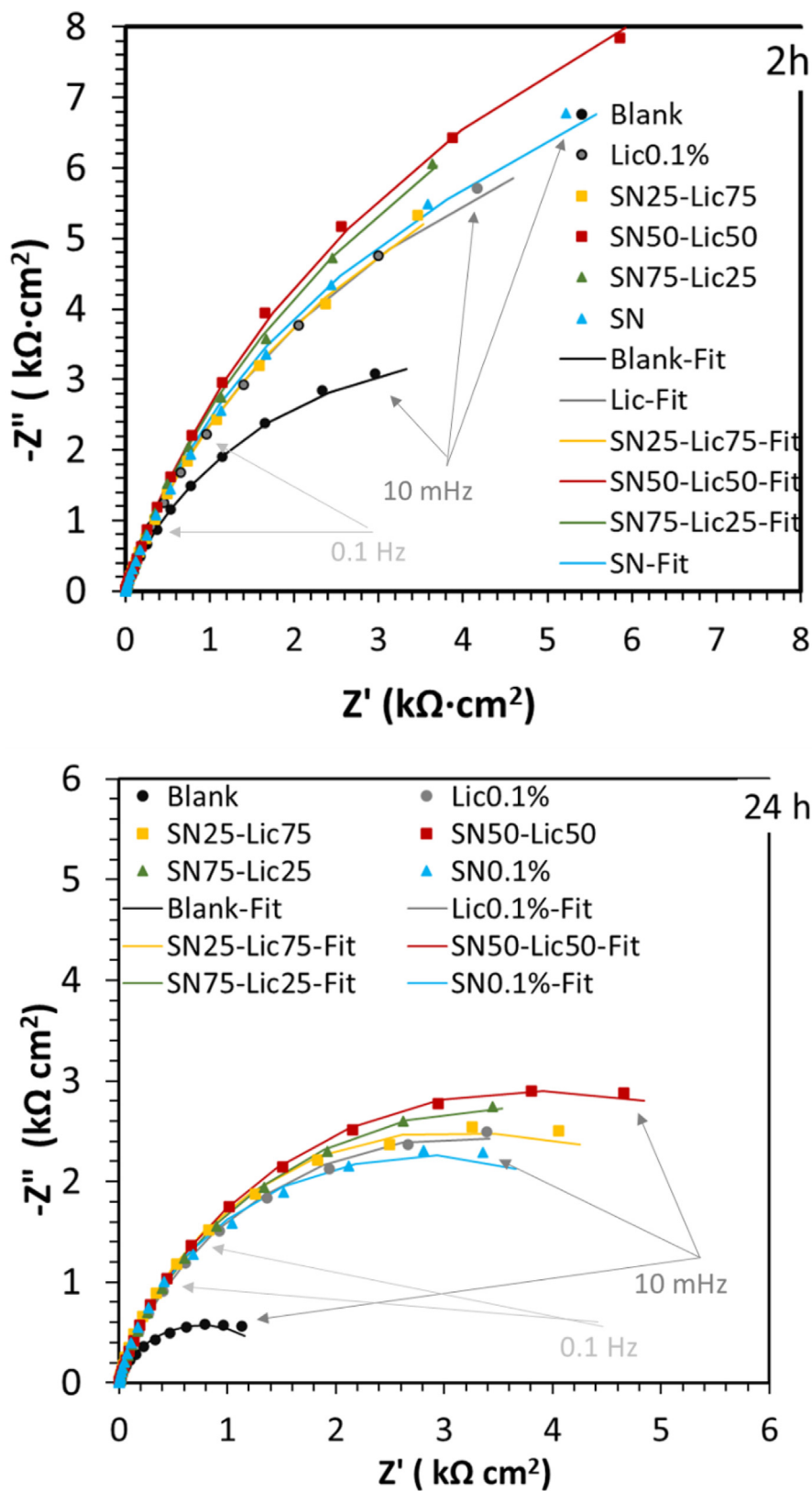


Fig. 3. Examples of the EIS test outputs for the ribbed steel after 2 and 24 h of exposure to the simulated concrete pore solutions with chlorides without and with different nitrite-licorice ratios. The experimental data are plotted with symbols and the fitted data with continuous lines.

regions inside the pits. It can be assumed that it occurs through a mechanism similar to that proposed for other compounds [45]. Comparing the results obtained in the different solutions under study, a certain synergic effect between licorice and nitrites can

be detected. For a fixed amount of addition, the one made up of similar proportions of the two inhibitors seems to be able to provide the lowest corrosion rate for the carbon steel bars in the simulated pore solution with chlorides.

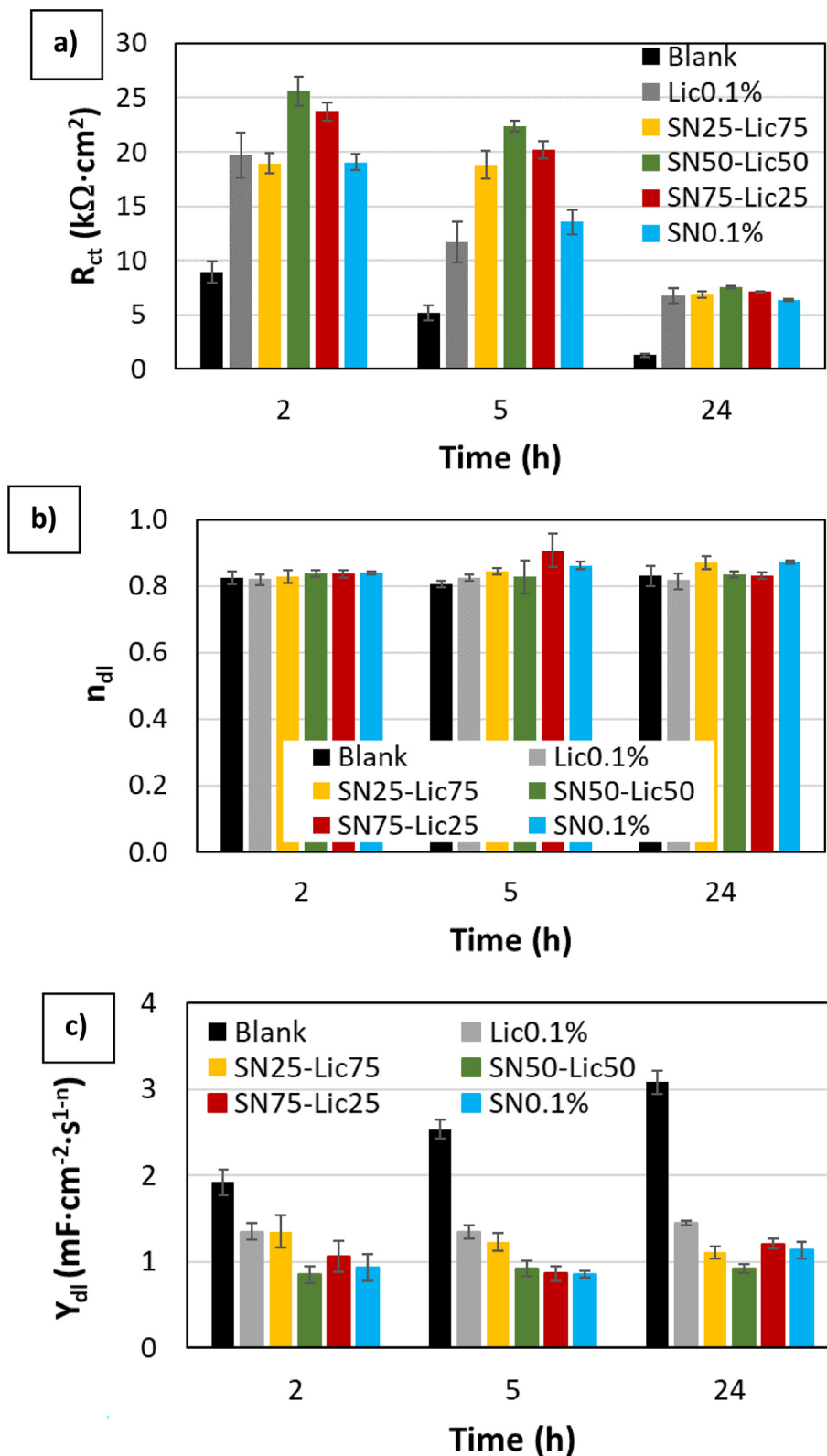


Fig. 4. Values obtained for parameters from the simulations of the EIS spectra of the corrugated steel bars after different times of immersion in the simulated pore solutions with and without inhibitors.

The parameters obtained from the simulations and related to CPE_{dl} also offer interesting information about the inhibiting process. While n_{dl} values (Fig. 4b) show no meaningful change, suggesting that no relevant alteration occurs in the double layer structure, interesting variations are observed in the values of Y_{dl}

(Fig. 4c). A decrease on Y_{dl} can be related to a decrease on the real corroding surface in the samples under study [49]. If both nitrites and licorice partially block the surface pits by an anodic inhibiting mechanism, the real corroding surface must decrease, and this must cause not only the reduction in the capacitive behavior of

the double layer but can also explain the lower R_{ct} values determined in inhibited solutions compared to the blank one for similar exposure times (Fig. 4a). The lowest Y_{dl} value obtained in SN50-Lic50 supports the hypothesis of an optimum synergic effect of this inhibitor mix. In other studies, it has been concluded that nitrite additions at low concentrations improve the adsorption of organic inhibitors, and synergy between nitrites and organic compounds can increase the ability of carbon steel in alkaline media with chloride to form passivating oxides [19].

On the other hand, from the analysis of the EIS spectra (Fig. 5), the efficiency of the different inhibitors in simulated pore solutions with chlorides can be calculated (Eq. (1)).

$$\text{Inhibitor effectiveness (\%)} = \left(\frac{R_{ct,inh} - R_{ct,b}}{R_{ct,inh}} \right) \times 100 \quad (1)$$

It can be seen that, although the R_{ct} of the steel in inhibited solutions decreases with time due to autocatalytic mechanism of the pitting attack [2], in the surface regions that are passivated/ blocked by the inhibitors, their efficiency, within the short time interval that can be considered for the solution test, is always increasing. That is to say, the attack progresses at a much lower rate in the presence of inhibitors than in their absence, while being relatively similar. Hence, though no other analysis different from the electrochemical measurements have been carried out, the sta-

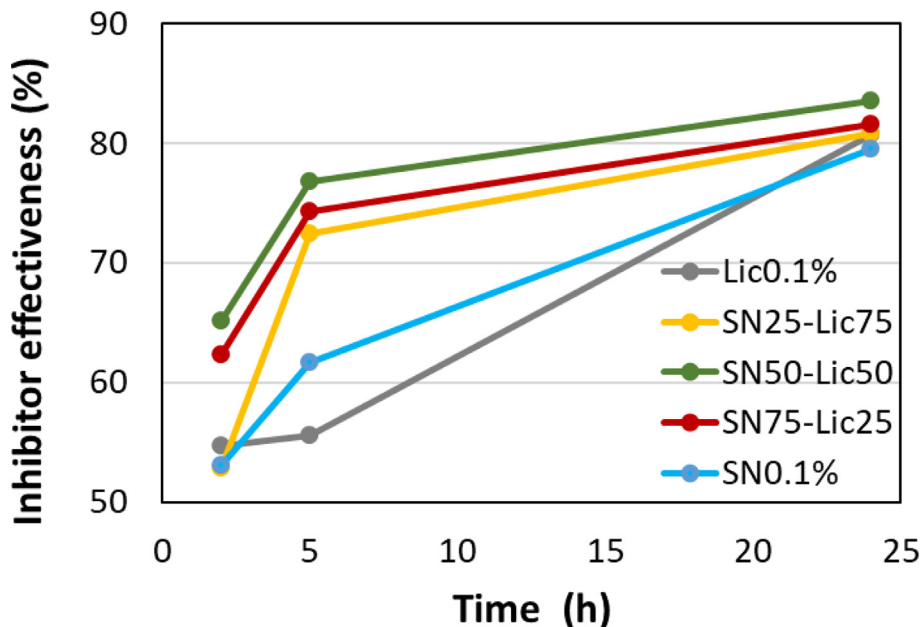


Fig. 5. The evolution of efficiency of the inhibitors in simulated pore solutions with chlorides. The plotted data have been calculated using the values plotted in Fig. 4a.

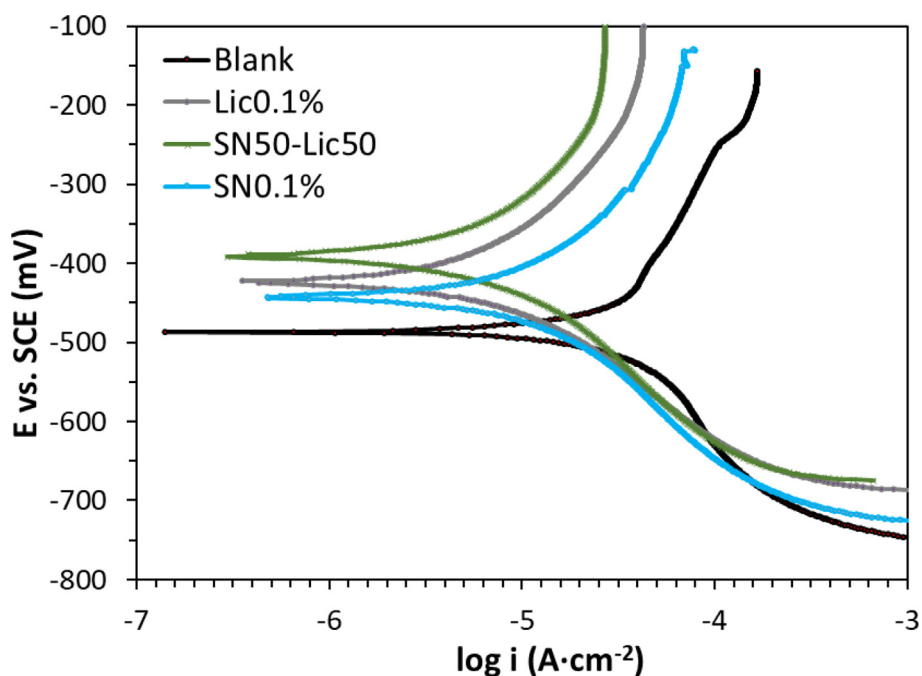


Fig. 6. Examples of the polarization curves of carbon steel ribbed bar immersed for 24 h in simulated pore solutions with chlorides.

bility of performance of the inhibitors over the testing time seems to be adequate and no undesired process seems to take place during the period considered. The simultaneous use of both inhibitors fosters the effectiveness of the mixes, pointing to a synergic mechanism for blocking the anodic areas of the pits. Again, the SN50-Lic50 seems to be a mix with potential inhibiting advantages if its effectiveness is considered.

To complete the electrochemical information obtained in solution, polarization curves of bars immersed 24 h in solutions without inhibitors and with 0.1% of licorice, nitrite and SN50-Lic50 mix were performed. Examples from the obtained curves can be seen in Fig. 6. The corrosion rates calculated from the polarization curves can be seen in Table 2, expressed as corrosion current densities (i_{corr}) and as mass loss rates. The results from the analysis of the polarization curves (Table 2) confirm that, after several hours,

the addition of Lic0.1% reduces the corrosion rate somehow more effectively than the addition of SN0.1%. SN50-Lic50 seems to be slightly more effective for reducing the corrosion rate after 24 h of immersion in simulated pore solutions with chlorides than the non-mixed licorice. The shift of the corrosion potential (E_{corr}) through higher values with the three inhibitory additions, is coherent with OCP measurements (Fig. 2) and confirms that the mechanism for all of them is predominantly anodic.

For the inhibitors under study, if the values of the anodic (β_a) and the cathodic (β_c) Tafel slopes are compared (Table 2), it can be seen that the corrosion rate takes place through a mixed mechanism whose control has a slight predominance of the anodic values ($\beta_a > \beta_c$). Moreover, the decrease in the i_{corr} values cannot be identified with an increase of the β_a in the anodic solutions (Table 2), but with a shift of the anodic branches of

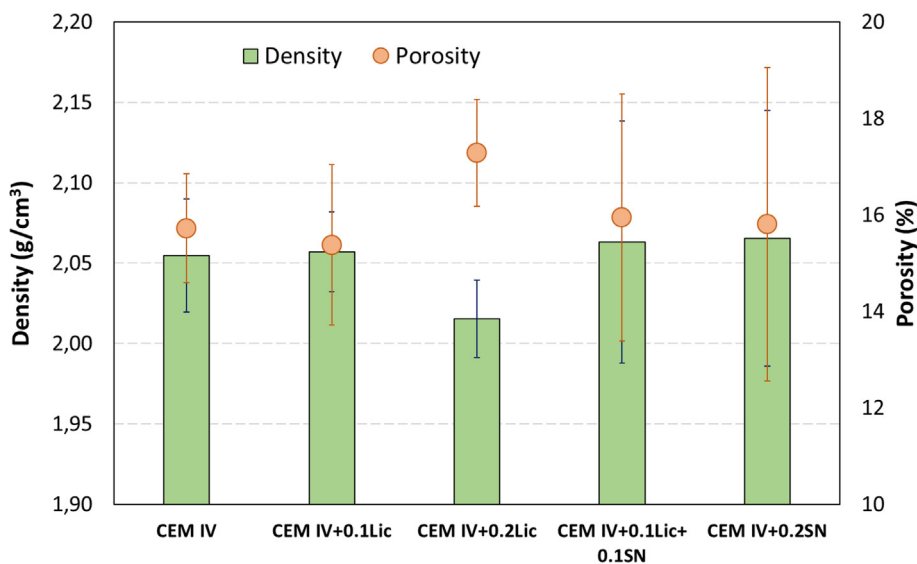


Fig. 7. Effect of the inhibitor on the porosity and the density of the mortar.

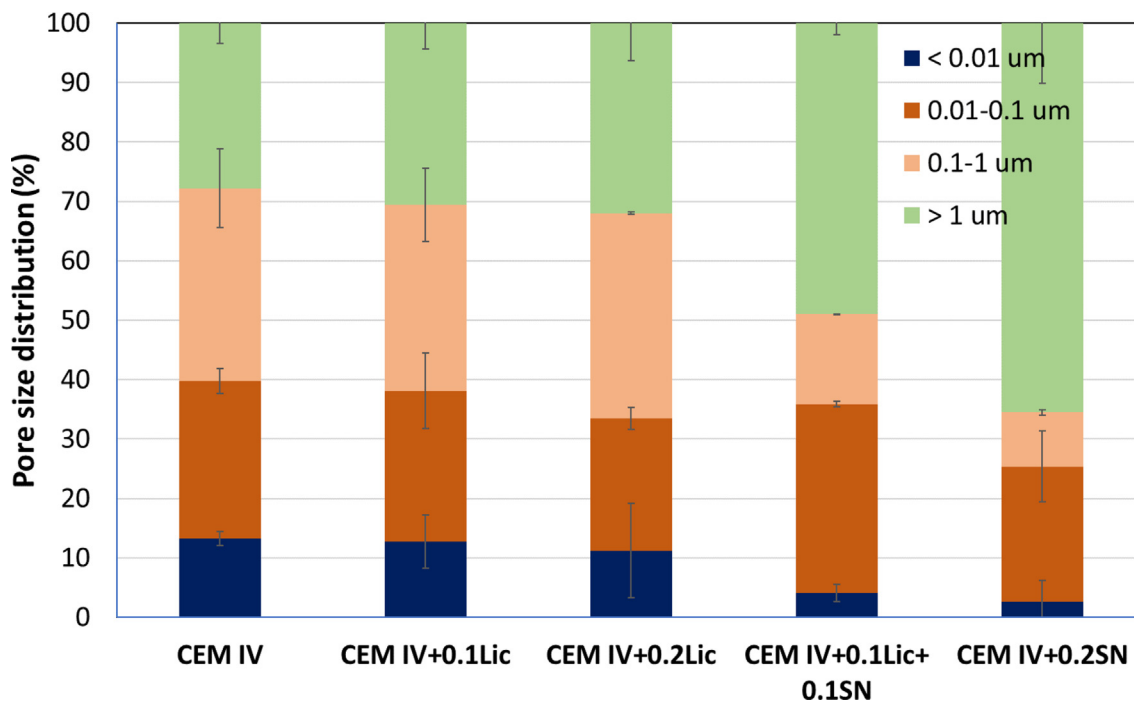


Fig. 8. Effect of the inhibitor on the pore size distribution in the mortars.

the curves through higher potentials (Fig. 6). This phenomenon indicates that the anodic process has not become more hindered in its global development, but the areas where this semi-reaction takes place have decreased. That is to say, some pits have become inactive due to the formation of passive oxide (when nitrites have been added) and/or precipitation of organic compounds (in the presence of licorice), while others remain essentially unaffected.

Effect of the inhibitor addition on the physical and mechanical properties of the mortars

Beside the positive electrochemical results reported in Section 3.1, before adding corrosion inhibitors to a reinforced mortar

structure, it is necessary to check their effect on the curing process of the binder and on its final mechanical properties and its porosity, to be sure that no relevant undesired side-effects occur.

In Fig. 7, the porosity and the density of mortars without and with inhibitors are compared. It can be seen that 0.1% licorice additions do not affect at all either the density or the porosity of the CEM IV mortars. The increase of the licorice addition up to 0.2% could already have had a small negative effect on the development of the curing process, as some small increase in the porosity and a slight reduction of the density could be guessed. After the 28-day curing period, the porosity of the mortar with a 0.2% of licorice is slightly higher than that of CEM IV mortar without inhibitors (Fig. 7). On the other hand, the addition of 0.2% sodium nitrite does not affect these parameters.

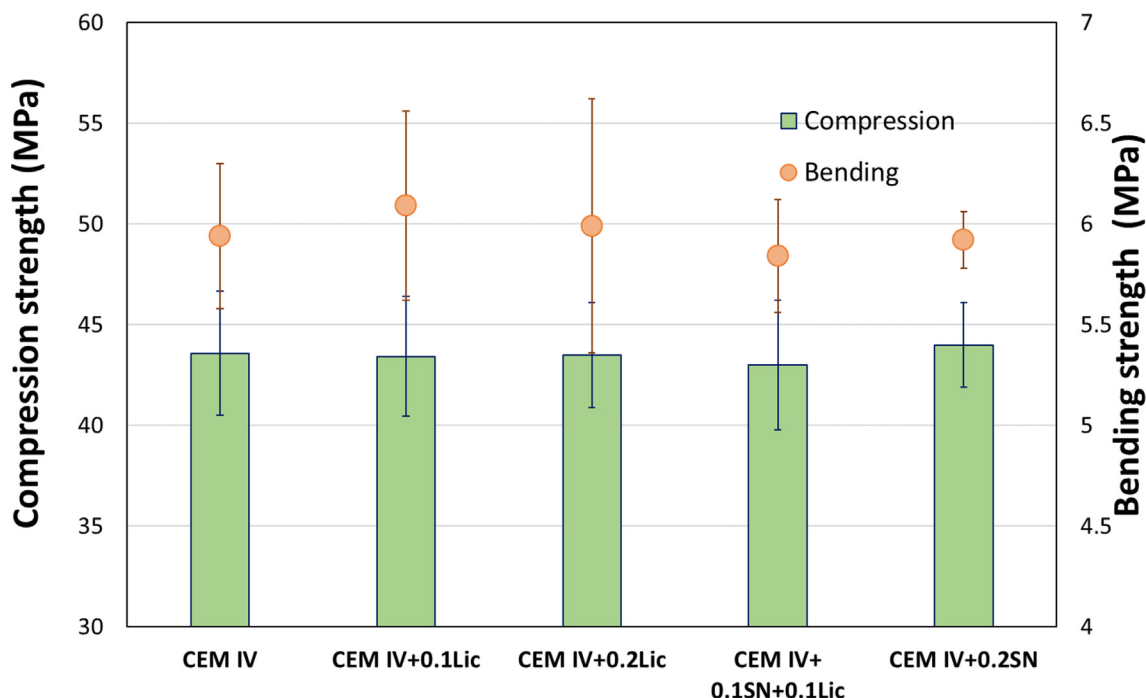


Fig. 9. Influence of the inhibitor addition on the compression strength and bending strength of the mortars.

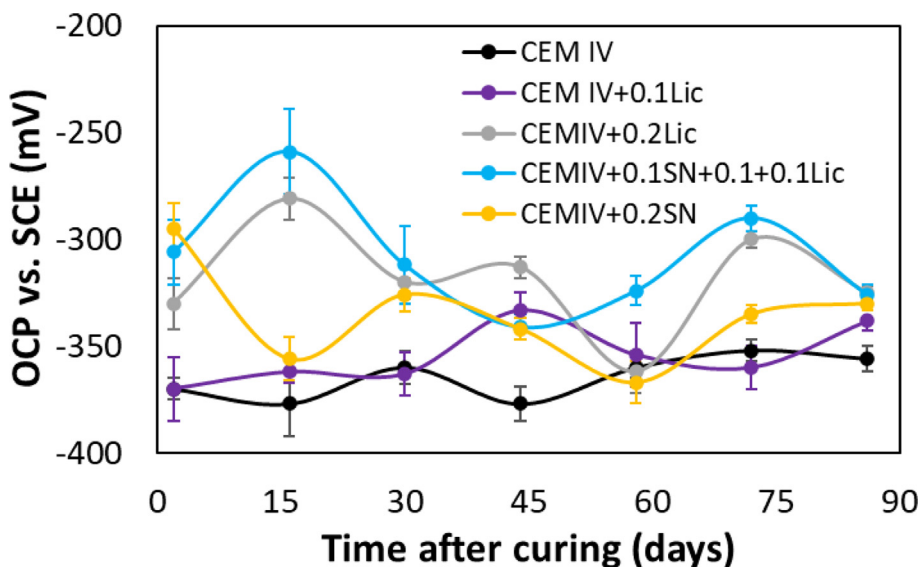


Fig. 10. Time evolution of the OCP of the reinforced steel bars embedded in mortar with and without inhibitors.

It can be seen in Fig. 8 that the pore size distribution is not meaningfully affected by the licorice additions, although a very slight increase of the percentage of higher diameter pores and a reduction of the fraction of the smallest pores (diameter < 0.1 μ m) could occur. A slightly higher fraction of big pores for the mortar with 0.2% licorice is coherent with the very slightly lower density determined for these mortars in comparison with that of CEM IV mortars (Fig. 7). On the other hand, although sodium nitrite additions do not affect the global volume of porosity in CEM IV mortar (Fig. 7), they affect the pore size distribution. The % of pores with a diameter greater than 1 μ m is higher in CEM IV + 0.1Lic + 0.1SN than in CEM IV, and the amount of big pores is still highest in CEM IV + 0.2SN mortar.

The effect of sodium nitrite on the mechanical properties reported in the previous published literature is controversial. In general, the presence of sodium nitrites in relevant amounts is considered detrimental [42]. Sodium nitrite affects the formed hydration products, as it increases sulphoaluminate presence, reducing the mechanical strength of the samples with a high amount of additions when compared to non-inhibited materials [50]. However, a negligible [51] or even positive [52] influence of sodium nitrite additions has even been reported by other authors. The results obtained in the present study (Fig. 9), which resort to very small inhibitory additions, demonstrate that no meaningful decrease in the mechanical properties of CEM IV occurs in any case, and that the change in the pore size distribution observed after

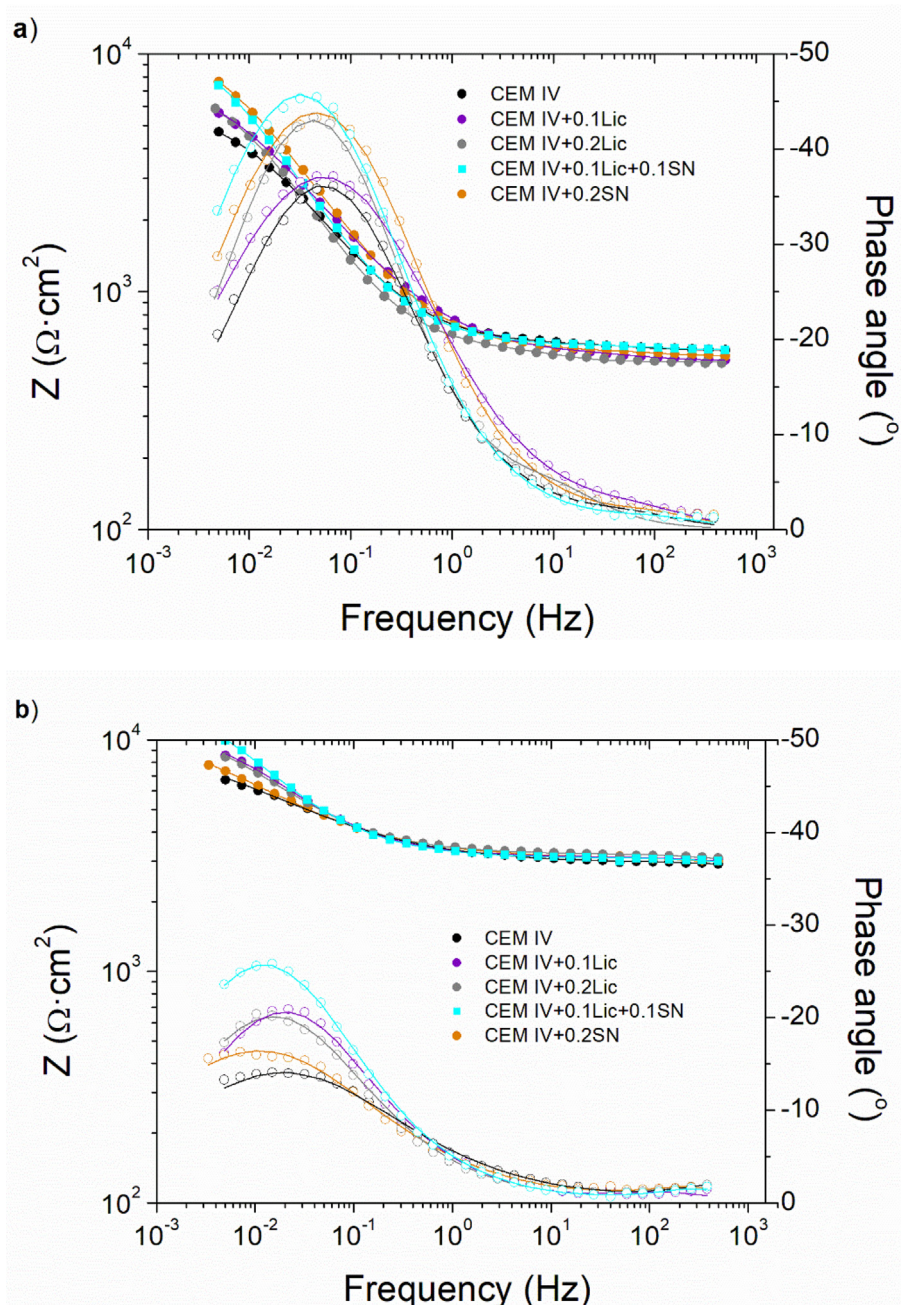


Fig. 11. Examples of the Bode plots of EIS spectra corresponding to reinforced mortar samples containing licorice and sodium nitrite during exposure to high humidity environment: a) 2 days after curing; b) 86 days after curing. Experimental data are plotted with symbols and fitted data with continuous lines.

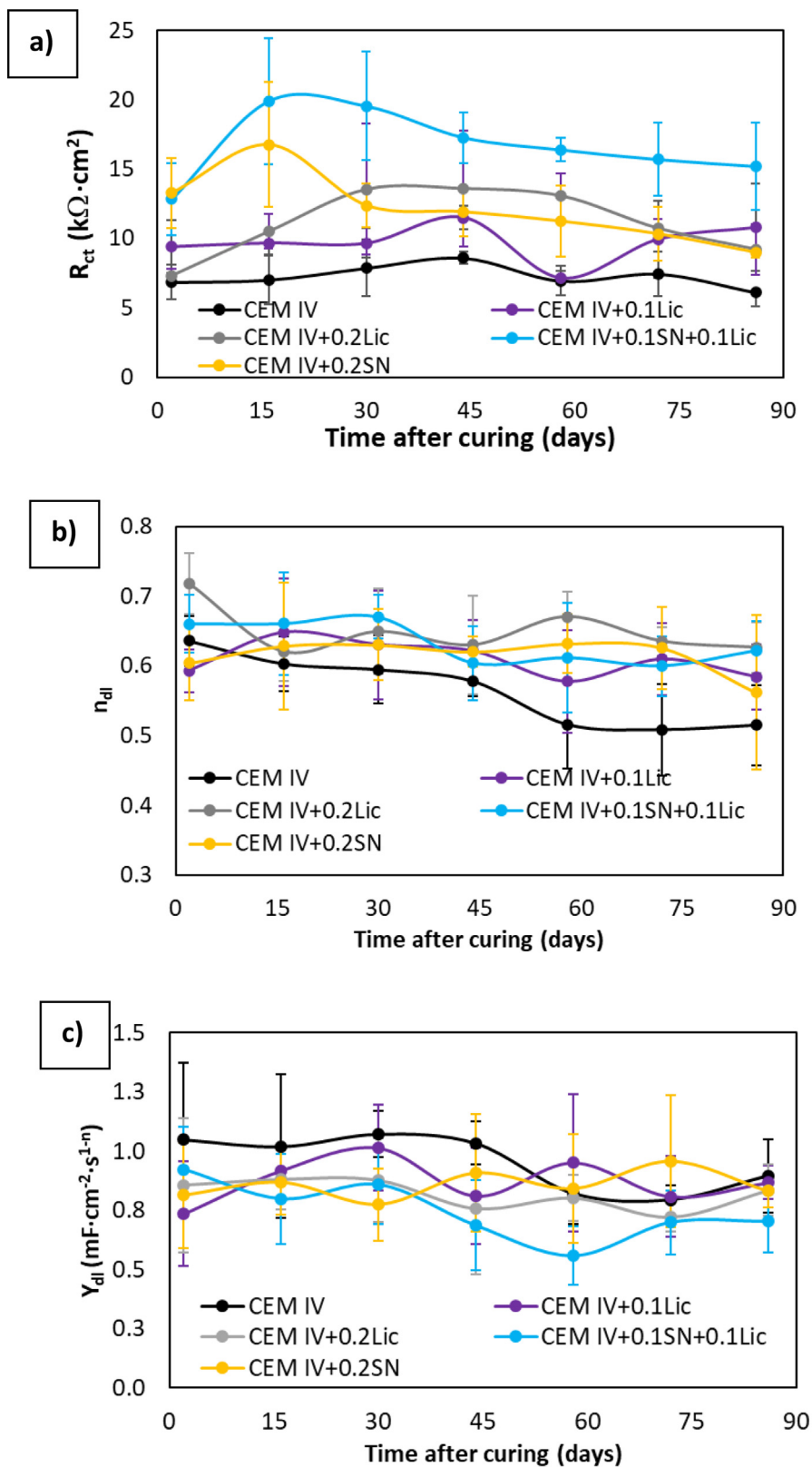


Fig. 12. Time-evolution of the values obtained for the parameters related with the low-frequency time constant of the EIS spectra corresponding to the reinforced mortar samples.

nitrite additions up to 0.2% (Fig. 8) is not enough to affect the mechanical behavior of the mortars and future in-service performance of concrete structures.

Effect of the inhibitor additions on the electrochemical performance of the steel in mortar

In Fig. 10, the time evolution of OCP values determined for the reinforced mortar samples can be seen. The differences between the OCP evolution in the different mortars are not very relevant, but it can be seen that the blank mortar tends to have lower OCP than the inhibited mortars, with the CEM IV + 0.1Lic + 0.1SN and CEM IV + 0.2Lic showing slightly higher values than the other reinforced mortars under study. The values of all the measured OCP always suggest active behaviors, except for CEMIV + 0.1Lic + 0.1SN after 15 days of exposure, where the synergic effect of both tested inhibitors seems to be able to shift the OCP to the corrosion uncertainty region.

The changes in the electrochemical behavior of the different reinforced mortars have also been monitored with EIS. Examples of the obtained spectra plotted as Bode diagrams can be seen in Fig. 11. Those experimental spectra have been simulated using an equivalent circuit with two cascade time-constants: $R_m(C_{ox}R_{ox}(-CPE_{dl}R_{ct}))$, where R_m is the resistance of the mortars surrounding the reinforcing carbon steel bar and C_{ox} and R_{ox} are, respectively, the capacitive behavior and the resistance of the oxides formed on the bar surfaces during curing and exposure. This equivalent circuit has already demonstrated its effectiveness to simulate the behavior of corrosion carbon steel bars in mortars [53]. The fitted spectra obtained using this equivalent circuit are plotted as contin-

uous lines in Fig. 11. The numerical values obtained from the fitting and related to the low-frequency time constant (which is clearly the one that controls the kinetics of the corrosion process in the mortars) are plotted in the images in Fig. 12, while the values corresponding to R_m and the electrochemical behavior of the oxides obtained by fitting can be seen in Table 3.

In Fig. 12a, the effective inhibitory synergy existing in CEM IV + 0.1Lic + 0.1SN becomes evident. The R_{ct} corresponding to this system are the highest during the exposure, so the corrosion rates of the embedded bars are the lowest. On the other hand, in the non-inhibited CEM IV, the reinforcing steel shows the lowest R_{ct} values, while the n_{dl} in mortars (Fig. 12b) show lower values than in solution (Fig. 4b). The decrease of n_{dl} values is typical of corroding carbon steel bars in this type of media when the attack has been developing over a certain period of time, as the heterogeneities in the mortar-steel increase. In this study, the decrease of n_{dl} with time can be seen for the inhibited CEM IV mortars (Fig. 12b), that is to say, the one which corrodes the fastest because of its lowest R_{ct} (Fig. 12a). Y_{dl} for the mortar specimens (Fig. 12c), as has been previously observed in solution tests when these inhibitors are used (Fig. 4), is somewhat lower for the systems where the R_{ct} is higher, suggesting that the inhibition mechanism proposed in Section 3.1 after solution studies can also be valid for mortars.

In Table 3, it can be seen that R_m is not affected at all by the addition of inhibitors. This result is coherent with the negligible differences detected between the porosity of the mortars under study (Fig. 7) and the identical mechanical behavior determined for all of them (Fig. 8). The increase of the mortar resistance over time can be related to different phenomena. On one hand, the CEM IV mortars are not completely cured after the usually estab-

Table 3

Values obtained from the simulation of the EIS spectra of reinforced mortar samples corresponding to the parameters related to the electrochemical performance of the mortar cover and oxides generated in the steel bar surfaces. χ^2 values obtained from the fitting are also included.

Mortar	Days	R_m ($k\Omega \cdot cm^2$)	R_{ox} ($k\Omega \cdot cm^2$)	C_{ox} ($mF \cdot cm^{-2}$)	χ^2
CEM IV	2	0.60 ± 0.08	0.09 ± 0.04	0.14 ± 0.05	(4 ± 1)·10 ⁻⁵
	16	0.78 ± 0.09	0.10 ± 0.06	0.3 ± 0.2	(6 ± 1)·10 ⁻³
	30	1.13 ± 0.08	0.11 ± 0.03	0.15 ± 0.04	(2.0 ± 0.7)·10 ⁻⁴
	44	1.44 ± 0.08	0.10 ± 0.05	0.14 ± 0.01	(3.4 ± 0.6)·10 ⁻⁴
	58	2.5 ± 0.2	0.14 ± 0.06	0.17 ± 0.03	(2 ± 1)·10 ⁻⁴
	72	2.88 ± 0.06	0.20 ± 0.09	0.18 ± 0.03	(1.1 ± 0.4)·10 ⁻⁴
CEM IV + 0.1Lic	2	0.54 ± 0.03	0.05 ± 0.01	0.12 ± 0.03	(3 ± 2)·10 ⁻⁴
	16	0.76 ± 0.04	0.06 ± 0.03	0.13 ± 0.05	(1.4 ± 0.6)·10 ⁻³
	30	1.14 ± 0.05	0.07 ± 0.02	0.10 ± 0.04	(1.1 ± 0.3)·10 ⁻³
	44	1.4 ± 0.1	0.05 ± 0.01	0.11 ± 0.03	(1.2 ± 0.8)·10 ⁻³
	58	2.2 ± 0.1	0.08 ± 0.03	0.08 ± 0.05	(1.4 ± 0.5)·10 ⁻³
	72	3.0 ± 0.1	0.10 ± 0.01	0.13 ± 0.02	(3.7 ± 0.5)·10 ⁻³
CEM IV + 0.2Lic	2	0.59 ± 0.09	0.10 ± 0.04	0.15 ± 0.04	(3.9 ± 0.8)·10 ⁻³
	16	0.8 ± 0.1	0.08 ± 0.07	0.20 ± 0.02	(1 ± 1)·10 ⁻²
	30	1.1 ± 0.1	0.12 ± 0.02	0.20 ± 0.06	(2 ± 1)·10 ⁻³
	44	1.4 ± 0.1	0.13 ± 0.02	0.13 ± 0.03	(2.6 ± 0.4)·10 ⁻³
	58	2.04 ± 0.05	0.15 ± 0.03	0.16 ± 0.05	(2.8 ± 0.6)·10 ⁻³
	72	2.73 ± 0.06	0.10 ± 0.02	0.14 ± 0.03	(2.3 ± 0.5)·10 ⁻³
CEM IV +0.1Lic +0.1SN	2	0.55 ± 0.03	0.08 ± 0.01	0.13 ± 0.05	(4.6 ± 0.9)·10 ⁻³
	16	0.78 ± 0.09	0.08 ± 0.03	0.23 ± 0.07	(3 ± 1)·10 ⁻³
	30	1.1 ± 0.1	0.12 ± 0.02	0.14 ± 0.03	(2.9 ± 0.3)·10 ⁻³
	44	1.2 ± 0.1	0.11 ± 0.04	0.10 ± 0.03	(3 ± 1)·10 ⁻³
	58	2.0 ± 0.1	0.12 ± 0.05	0.08 ± 0.03	(2.4 ± 0.9)·10 ⁻³
	72	3.0 ± 0.1	0.09 ± 0.04	0.10 ± 0.02	(2 ± 1)·10 ⁻³
CEM IV +0.2SN	2	0.61 ± 0.08	0.14 ± 0.06	0.09 ± 0.03	(2.9 ± 0.8)·10 ⁻³
	16	0.84 ± 0.07	0.09 ± 0.04	0.23 ± 0.07	(4 ± 1)·10 ⁻³
	30	1.1 ± 0.1	0.10 ± 0.06	0.09 ± 0.03	(3.5 ± 0.9)·10 ⁻³
	44	1.41 ± 0.05	0.11 ± 0.03	0.17 ± 0.03	(2.1 ± 0.9)·10 ⁻³
	58	2.23 ± 0.06	0.10 ± 0.05	0.14 ± 0.03	(1.8 ± 0.7)·10 ⁻³
	72	2.79 ± 0.06	0.10 ± 0.05	0.10 ± 0.03	(2.4 ± 0.8)·10 ⁻³
86	3.2 ± 0.1	0.14 ± 0.06	0.08 ± 0.03	(2.7 ± 0.8)·10 ⁻³	
86	3.2 ± 0.1	0.14 ± 0.1	0.09 ± 0.03	(2.4 ± 0.4)·10 ⁻³	
86	3.2 ± 0.1	0.14 ± 0.1	0.09 ± 0.03	(2.3 ± 0.9)·10 ⁻³	

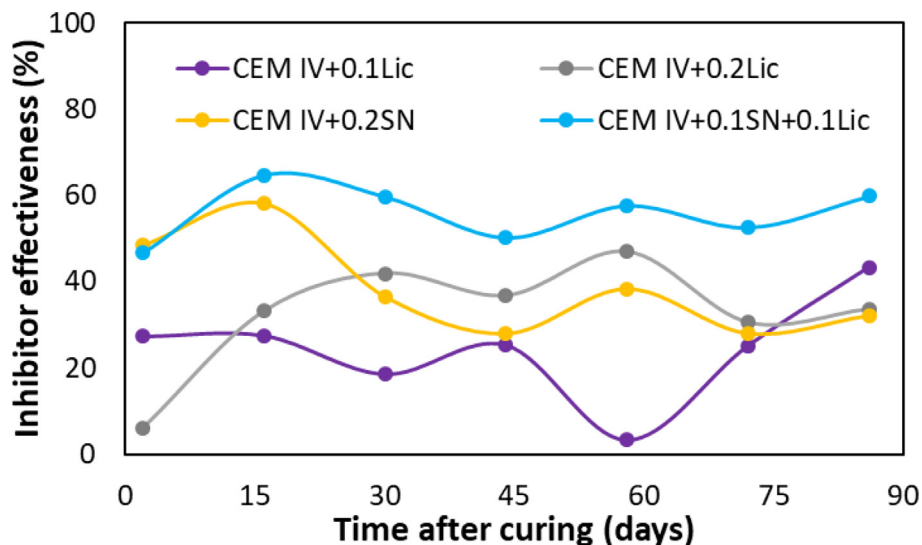


Fig. 13. Effectiveness calculated from the EIS measurements for the different inhibitors tested in mortar with chlorides. The plotted data have been calculated using the values plotted in Fig. 12a.

lished 28-day curing period [8]. Moreover, at RH, like the ones used for the test, after a certain time, part of the water contained in the pores of the mortars can be lost. The contribution of this phenomena could help to understand the steeper increase in the mortar resistances monitored between approximately 40 and 80 days of exposure after the curing period.

On the other hand, in Table 3, it can be observed that, for given systems, R_{ox} tends to increase with time, which is coherent with its identification with oxide resistance on the bar surface. In spite of the unavoidable uncertainty related to parameters of this medium-frequencies time-constant, it can be said that the R_{ct} for the CEM IV system is higher than for the inhibited ones, and that this parameter tends to be lower for CEM IV + 0.1Lic + 0.1SN than for other systems. The capacitances of the oxides, C_{ox} , which has been simulated with an ideal capacitor, always exhibit values around $10^{-4}F/cm^2$. In this specific case with high overlapping, the use of CPE at medium frequencies complicates the simulation and sometimes produces anomalous values.

The χ^2 values in Table 3 confirm the accuracy of the fitting already suggested by the good matching between the experimental data (symbols) and the fitted data (lines) in Fig. 11. So, the adequacy of the equivalent circuit used for the simulation is proved.

The evolution of efficiencies of the different inhibitors (Eq. (1)) in mortars during the three-month testing period can be seen in Fig. 13. These data have been calculated from resistances associated to the low-frequency time constant (Fig. 12a) as they are much higher than those corresponding to the medium frequency time constant (R_{ox} in Table 3) and, hereafter, they are the ones that control the kinetics of the corrosion processes under study. Results in Fig. 13 show that, after curing, the effectiveness of the inhibitors under study remains relatively stable during the subsequent months. The results highlight the interest of non-toxic 0.2% licorice additions in comparison with toxic 0.2% nitrite additions, as the effectiveness of both additions can be comparable. Moreover, the effectiveness of the 50% licorice and 50% sodium nitrite is again observed.

Conclusions

The most relevant conclusions that can be drawn from the results of the present contribution can be summarized as follows:

- Tests in simulated pore solutions with chlorides inform that the licorice is able to act as an anodic inhibitor with an effectiveness comparable to that of nitrite ions. This organic green compound reduces the corrosion rate through a reduction of the actively corroding area of the carbon steel rebars.
- The additions of licorice in reduced amounts do not affect the porosity, pore size distribution and mechanical properties of the cured mortars.
- The 0.1 and 0.2% licorice additions to chloride-contaminated CEM IV mortars prove to be enough to reduce the corrosion rate in steel in mortars contaminated with amounts of Cl^- as high as 0.8% in relation to the cement weight. Moreover, the inhibitory additions are durable in mortar, as their effectiveness remain stable for months after curing.
- The results obtained in mortar demonstrate the interest of non-toxic 0.2% licorice additions in comparison with toxic 0.2% nitrite additions, as the effectiveness of both inhibitors can be comparable.
- Licorice has shown a synergic inhibitory action with nitrite. The inhibitory 50% licorice + 50% nitrite mix has demonstrated especially interesting properties for the corrosion control of the steel in chloride contaminated concrete, as has been proved both in solution and in mortar studies.
- In mortars with 0.8% chlorides and 0.2% inhibitors, both related to the cement weight, the 50% licorice + 50% nitrite mix shows an inhibitory effectiveness of 55–60%, while sodium nitrite has effectiveness of about 35% during the second and third months of testing.

Declaration of Competing Interest

The authors declare that they have no known competing financial interests or personal relationships that could have appeared to influence the work reported in this paper.

Acknowledgements

This research was funded by the European Union Horizon 2020 Research and Innovation MSCA-IF-2019 Programme under grant agreement No. 892074 (NATCON project). Support from PID2021-

1258100B-C22 project, financed by MCIN/AEI/10.13039/501100011033/ and FEDER, and funding for APC: Universidad Carlos III de Madrid (Agreement CRUE-Madroño 2023) are also acknowledged.

References

- [1] M. Stefanoni, U. Angst, B. Elsener, *Cem. Concr. Res.* 103 (2018) 35–48, <https://doi.org/10.1016/j.cemconres.2017.10.007>.
- [2] J.A. González, E. Otero, S. Feliu, A. Bautista, E. Ramírez, P. Rodríguez, W. López, *Mag. Concr. Res.* 50 (1998) 189–199, <https://doi.org/10.1680/macrc.1998.50.3.189>.
- [3] A. Bautista, J.C. Pomares, M.N. González, F. Velasco, *Constr. Build. Mater.* 229 (2019), <https://doi.org/10.1016/j.conbuildmat.2019.116899>.
- [4] Y. Ma, Z. Guo, L. Wang, J. Zhang, *Constr. Build. Mater.* 152 (2017) 240–249, <https://doi.org/10.1016/j.conbuildmat.2017.06.169>.
- [5] E. Moreno, A. Cobo, A. Palomo, M.N. González, *Constr. Build. Mater.* 61 (2014) 156–163, <https://doi.org/10.1016/j.conbuildmat.2014.03.003>.
- [6] J.K. Das, B. Pradhan, *J. Build. Eng.* 50 (2022), <https://doi.org/10.1016/j.job.2022.104192>.
- [7] E.Q. Zhang, Z. Abbas, L. Tang, *Constr. Build. Mater.* 185 (2018) 57–68, <https://doi.org/10.1016/j.conbuildmat.2018.07.025>.
- [8] A. Bautista, E.C. Paredes, F. Velasco, S.M. Alvarez, *Constr. Build. Mater.* 93 (2015) 350–359, [10.1016/j.conbuildmat.2015.04.060](https://doi.org/10.1016/j.conbuildmat.2015.04.060).
- [9] A. Bautista, E.C. Paredes, S.M. Alvarez, F. Velasco, *Corros. Sci.* 102 (2016) 363–372, <https://doi.org/10.1016/j.corsci.2015.10.029>.
- [10] J.A. González, E. Ramírez, A. Bautista, *Cem. Concr. Res.* 28 (1998) 577–589, [https://doi.org/10.1016/S0008-8846\(98\)00014-3](https://doi.org/10.1016/S0008-8846(98)00014-3).
- [11] P. Garcés, P. Saura, E. Zornoza, C. Andrade, *Corros. Sci.* 53 (2011) 3991–4000, <https://doi.org/10.1016/j.corsci.2011.08.002>.
- [12] A. Ahmad, A. Kumar, *J. Inst. Eng. India Ser. D.* 98 (2017) 177–187, [10.1007/s40033-016-0125-9](https://doi.org/10.1007/s40033-016-0125-9).
- [13] Z. Chen, H. Ye, *Cem. Concr. Res.* 143 (2021), <https://doi.org/10.1016/j.cemconres.2021.106398>.
- [14] F. Bolzoni, A. Brenna, M. Ormellese, *Cem. Concr. Res.* 154 (2022), [10.1016/j.cemconres.2022.106719](https://doi.org/10.1016/j.cemconres.2022.106719).
- [15] Hw. Song, V. Saraswathy, S. Muralidharan, C.-H. Lee, K. Thangavel, *J. Appl. Electrochem.* 39 (2009) 15–22, <https://doi.org/10.1007/s10800-008-9632-1>.
- [16] X. Li, L. O'Moore, S. Wilkie, Y. Song, J. Wei, P.L. Bond, Z. Yuan, L. Hanzic, G. Jiang, *Constr. Build. Mater.* 233 (2020), <https://doi.org/10.1016/j.conbuildmat.2019.117341>.
- [17] J.O. Okeniyi, A.P.I. Popoola, C.A. Loto, O.A. Omotosho, S.O. Okpala, I.J. Ambrose, *Adv. Mater. Sci. Eng.* (2015), <https://doi.org/10.1155/2015/540395>.
- [18] P. Xu, J. Zhou, G. Li, P. Wang, P. Wang, F. Li, B. Zhang, H. Chi, *Constr. Build. Mater.* 288 (2021), <https://doi.org/10.1016/j.conbuildmat.2021.123101>.
- [19] M. Johari, S.R. Allahkaram, F. Teymouri, I. Azamian, M. Shekarchi, *Constr. Build. Mater.* 308 (2021), <https://doi.org/10.1016/j.conbuildmat.2021.125037>.
- [20] Y.P. Asmara, T. Kurniawan, A.G.E. Sutjipto, J. Jafar, *Indones. J. Sci. Technol.* 3 (2018) 158–170, [10.17509/ijost.v3i2.12760](https://doi.org/10.17509/ijost.v3i2.12760).
- [21] P.B. Raja, M.G. Sethuraman, *Mater. Lett.* 62 (2008) 113–116, <https://doi.org/10.1016/j.matlet.2007.04.079>.
- [22] L.T. Popoola, *Corros. Rev.* 37 (2019) 71–102, <https://doi.org/10.1515/corrrev-2018-0058>.
- [23] E. Salehi, R. Naderi, B. Ramezanzadeh, *Appl. Surf. Sci.* 396 (2017) 1499–1514, <https://doi.org/10.1016/j.apsusc.2016.11.198>.
- [24] B. Liao, Z. Luo, S. Wan, L. Chen, *J. Ind. Eng. Chem.* 117 (2023) 238–246, <https://doi.org/10.1016/j.jiec.2022.10.010>.
- [25] F. Kaya, R. Solmaz, I.H. Geçibesler, *J. Ind. Eng. Chem.* 122 (2023) 102–117, <https://doi.org/10.1016/j.jiec.2023.02.013>.
- [26] R. Anitha, S. Chitra, V. Hemapriya, I.M. Chung, S. Kim, M. Prabakara, *Constr. Build. Mater.* 213 (2019) 246–256, <https://doi.org/10.1016/j.conbuildmat.2019.04.046>.
- [27] Y. Liu, Z. Song, W. Wang, L. Jiang, Y. Zhang, M. Guo, F. Song, N. Xu, *J. Clean. Prod.* 214 (2019) 298–307, <https://doi.org/10.1016/j.jclepro.2018.12.299>.
- [28] S. Shanmugapriya, P. Prabhakar, S. Rajendran, *Mater. Today: Proc.* 5 (2018) 8789–8795, <https://doi.org/10.1016/j.matpr.2017.12.307>.
- [29] D.B. Left, M. Zertoubi, S. Khoudali, M. Azzi, *Electrochim. Acta* 36 (2018) 249–257, <https://doi.org/10.4152/pea.201804249>.
- [30] M. Ben Harba, S. Abubshait, N. Etteyeb, M. Kamoun, A. Dhoui, *Arab. J. Chem.* 13 (2020) 4846–4856, <https://doi.org/10.1016/j.arabjc.2020.01.016>.
- [31] Q. Liu, Z. Song, H. Han, S. Donkor, L. Jiang, W. Wang, H. Chu, *Constr. Build. Mater.* 260 (2020), <https://doi.org/10.1016/j.conbuildmat.2020.119695>.
- [32] Q. Wang, X. Wu, H. Zheng, L. Liu, Q. Zhang, A. Zhang, Z. Yan, Y. Sun, Z. Li, X. Li, *J. Build. Eng.* 63B (2023), <https://doi.org/10.1016/j.job.2022.105568>.
- [33] N. Etteyeb, X.R. Nóvoa, *Corros. Sci.* 112 (2016) 471–482, <https://doi.org/10.1016/j.corsci.2016.07.016>.
- [34] S.P. Palanisamy, G. Maheswaran, A. Geetha Selvarani, C. Kamal, G. Venkatesh, *J. Build. Eng.* 19 (2018) 376–383, <https://doi.org/10.1016/j.job.2018.05.020>.
- [35] I. Pradipta, D. Kong, J.B.L. Tan, *Constr. Build. Mater.* 221 (2019) 351–362, <https://doi.org/10.1016/j.conbuildmat.2019.06.006>.
- [36] J. Wang, J. Zhao, M. Tabish, L. Peng, Q. Cheng, F. Shi, *J. Ind. Eng. Chem.* 122 (2023) 102–117, <https://doi.org/10.1016/j.jiec.2022.12.037>.
- [37] L. Siracusa, A. Saija, M. Cristani, F. Cimino, M. D'Arrigo, D. Trombetta, F. Rao, G. Ruberto, *Fitoterapia* 82 (2011) 546–556, <https://doi.org/10.1016/j.fitote.2011.01.009>.
- [38] A. Dal Bosco, S. Mattioli, Z. Matics, Z. Szendrő, Z. Gerencsér, A. Cartoni Mancinelli, M. Kovács, M. Cullere, C. Castellini, A. Dalle Zotte, *Meat Sci.* 158 (2019), [10.1016/j.meatsci.2019.107921](https://doi.org/10.1016/j.meatsci.2019.107921).
- [39] E. Alibakhshi, M. Ramezanzadeh, G. Bahlakeh, B. Ramezanzadeh, M. Mahdavian, M. Motamedi, *J. Molec. Liq.* 255 (2018) 185–198, <https://doi.org/10.1016/j.molliq.2018.01.144>.
- [40] E. Alibakhshi, M. Ramezanzadeh, S.A. Haddadi, G. Bahlakeh, B. Ramezanzadeh, M. Mahdavian, *J. Clean. Prod.* 210 (2019) 660–672, [10.1016/j.jclepro.2018.11.053](https://doi.org/10.1016/j.jclepro.2018.11.053).
- [41] R. Naderi, A. Bautista, F. Velasco, M. Soleimani, M. Pourfath, *J. Molec. Liq.* (2021) 117856, <https://doi.org/10.1016/j.molliq.2021.117856>.
- [42] C. Pan, N. Chen, J. He, S. Liu, K. Chen, P. Wang, P. Xu, *Constr. Build. Mater.* 260 (2020) 11972, <https://doi.org/10.1016/j.conbuildmat.2020.119724>.
- [43] I. Lapiro, G. Zur, E. Ofer-Rozovsky, K. Kovler, *Mater. Today: Proc.* (2023) in press, <https://doi.org/10.1016/j.matpr.2023.06.095>.
- [44] J. Xu, J. Wei, G. Ma, Q. Tan, *Corros. Sci.* 176 (2020), <https://doi.org/10.1016/j.corsci.2020.108940>.
- [45] R. Naderi, A. Bautista, F. Velasco, M. Soleimani, M. Pourfath, *J. Build. Eng.* 58 (2022), <https://doi.org/10.1016/j.job.2022.105055>.
- [46] NRMCA TIP 13, “Chloride Limits in Concrete” (Silver Spring, MD: NRMCA).
- [47] P. Garcés, P. Saura, A. Méndez, E. Zornoza, C. Andrade, *Corros. Sci.* 50 (2008) 498–509, <https://doi.org/10.1016/j.corsci.2007.08.016>.
- [48] L. Dhoubi, P. Refait, E. Triki, J.M. Génin, *J. Mater. Sci.* 41 (2006) 4928–4936, <https://doi.org/10.1007/s10853-006-0332-0>.
- [49] C. Moral, A. Bautista, F. Velasco, *Corros. Sci.* 51 (2009) 1651–1657, <https://doi.org/10.1016/j.corsci.2009.04.017>.
- [50] R. Liu, Y. Wang, G. Sheng, Influence of sodium nitrite on the early strength of cement-fly ash composite cementitious material. 4th International Conference on Sensors, Measurement and Intelligent Materials (ICSMIM 2015).
- [51] V.S. Reddy, T. Prashanth, S.P. Raju V, P. Prashanth, Effect of organic and inorganic corrosion inhibitors on strength properties of concrete. 2nd International Conference on Design and Manufacturing Aspects for Sustainable Energy (ICMED 2020), E3S Web of Conferences 184 (2020) 01112, <https://doi.org/10.1051/e3sconf/202018401112>.
- [52] V. Madhavan, C. Antony Jeyasehar, *IJEAS* 5 (3) (2013) 11–25, <https://dergipark.org.tr/en/pub/ijeas/issue/23588/25120>.
- [53] S. Shagñay, A. Bautista, J. Donaire, M. Torres-Carrasco, D.M. Bastidas, F. Velasco, *Cem. Concr. Comp.* 130 (2022), <https://doi.org/10.1016/j.cemconcomp.2022.104557>.